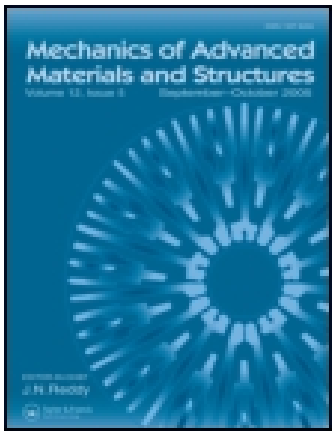

Mechanics of Advanced Materials and Structures
Publication details, including instructions for authors and subscription information:
http://www.tandfonline.com/loi/umcm20

Vibration Modeling of Multilayer Composite Structures with Viscoelastic Layers

K. Akoussan[a], H. Boudaoud[b], Daya El-Mostafa[ac] & E. Carrera[d]

[a] Laboratoire d'Etude des Microstructures et de Mécanique des Matériaux (LEM3), Université de Lorraine, Metz, France

[b] Equipe de Recherche des Processus Innovatifs (ERPI), Université de Lorraine, Nancy, France

[c] Laboratory of Excellence on Design of Alloy Metals for Low-Mass Structures ('DAMAS'), Metz, France

[d] Department of Aeronautics and Aerospace Engineering, Politecnico di Torino, Torino, Italy

Accepted author version posted online: 31 Aug 2014.Published online: 25 Sep 2015.

To cite this article: K. Akoussan, H. Boudaoud, Daya El-Mostafa & E. Carrera (2015) Vibration Modeling of Multilayer Composite Structures with Viscoelastic Layers, Mechanics of Advanced Materials and Structures, 22:1-2, 136-149, DOI: 10.1080/15376494.2014.907951

To link to this article: http://dx.doi.org/10.1080/15376494.2014.907951

Mechanics of Advanced Materials and Structures (2015) **22**, 136–149

ISSN: 1537-6494 print / 1537-6532 online
DOI: 10.1080/15376494.2014.907951

Taylor & Francis
Taylor & Francis Group

Vibration Modeling of Multilayer Composite Structures with Viscoelastic Layers

K. AKOUSSAN[1], H. BOUDAOUD[2], DAYA EL-MOSTAFA[1,3], and E. CARRERA[4]

[1]*Laboratoire d'Etude des Microstructures et de Mécanique des Matériaux (LEM3), Université de Lorraine, Metz, France*
[2]*Equipe de Recherche des Processus Innovatifs (ERPI), Université de Lorraine, Nancy, France*
[3]*Laboratory of Excellence on Design of Alloy Metals for Low-Mass Structures ('DAMAS'), Metz, France*
[4]*Department of Aeronautics and Aerospace Engineering, Politecnico di Torino, Torino, Italy*

Received 21 February 2014; accepted 20 March 2014.

This work deals with the vibration of orthotropic multilayer sandwich structures with viscoelastic core. A finite element model is derived from a classical zigzag model with shear deformation in the viscoelastic layer. The aim of the present work is to establish numerical models and develop numerical tools to design multilayer composites structures with high damping properties. To fulfill this purpose, a finite element model has been developed for vibration analysis of a sandwich plate (elastic orthotropic)/(viscoelastic orthotropic)/(elastic orthotropic). A numerical study from the variation of the damping properties of the structures was performed according to the faces materials fibers orientation.

Keywords: vibration, sandwich, orthotropic, viscoelastic, plate, asymptotic numerical method

1. Introduction

Sandwich plates with a viscoelastic core have been recognized to be useful for reducing and controlling vibration response of lightweight and flexible structures in numerous sectors: aerospace, automobile, and civil engineering. Since 1959 and the work of Kerwin [1], an intensive research work was devoted to this type of structures. Initially, analytical methods were developed to yield approximate damping properties (i.e., modal loss factor and natural frequency) of sandwich beam and plate structures with simple boundary conditions [2–4].

Recently, Bilasse et al. [5] developed a model in the finite element framework to determine the damping properties of a three isotropic layer sandwich beam and plate with viscoelastic core, by solving the free vibration problem. The modeling by the finite element method of viscoelastic sandwich structures induces nonlinear problems involving the frequency dependent stiffness matrix. Thus, the determination of damping properties is not direct and it cannot be usually performed by commercial codes. Several numerical strategies have been developed, such as the modal strain energy technique [6], the QR method [7], an approximate asymptotic method [3], the iterative order-reduction-iteration method [8], and the asymptotic numerical methods (ANM) [9, 10]. We refer to Boudaoud et al. [10] and Bilasse et al. [11] for a detailed overview presenting advantages and drawbacks of these methods. Of course, the numerical analysis of sandwich structures requires also the account of the transverse shear in the viscoelastic layer to predict accurately the structural damping. This transverse shear is mainly due to the difference between in-plane displacements of the elastic layers and to the low stiffness of the core. This cannot be accounted for within a standard beam or shell models. Hence, the use of layer-wise or zig-zag models is the most appropriate solution that can obtain a reasonable computational cost. An essential review of applied theories and models for sandwich structures can be found in Hu et al. [12] and Carrera [13].

For a few years, the benefits of components and products designed and produced in composite materials instead of metals, are well recognized by many industries. All of the former studies that were limited to sandwich structures with isotropic layers have to be extended.

To this end, Araùjo et al. [14, 15] used a mixed layerwise theory for anisotropic laminate plates with viscoelastic core in finite element formulation. More recently, Ferreira et al. [16] used a layer-wise finite element model for the analysis of sandwich laminated plates with a viscoelastic core and laminated anisotropic face layers, where the stiffness and mass matrices are obtained by Carrera's Unified Formulation (CUF) [17, 18]. Berthelot and Sefrani [19, 20], on the other hand, used the Ritz energy method to determine the loss factor of multilayered plates and beams with or without viscoelastic

Address correspondence to K. Akoussan, Laboratoire d'Etude des Microstructures et de Mécanique des Matériaux, Université de Lorraine, UMR CNRS 7239, Ile du Saulcy, Metz 57045, France. E-mail: Komlan.akoussan@univ-lorraine.fr
Color versions of one or more of the figures in the article can be found online at www.tandfonline.com/umcm.

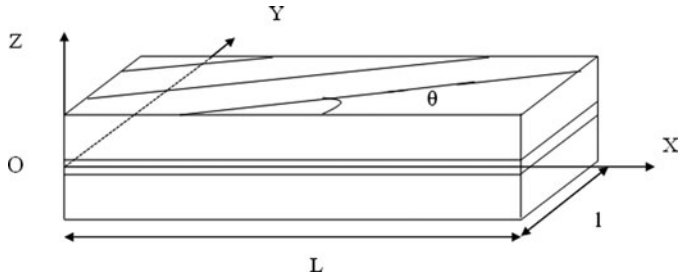

Fig. 1. Global face fibers orientation.

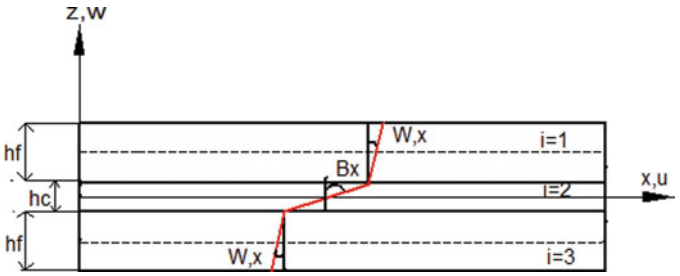

Fig. 2. Displacement field for the sandwich structure.

core for very specific boundary conditions. They studied the optimal design of symmetrical laminated thin plates comprised of fiber-reinforced layers and viscoelastic layers by varying the material fibers orientation. Their work was recently generalized to other boundary conditions by Li and Narita [21]. Adams and Maheri [22] investigated damping of angle-ply laminates made of unidirectional glass or carbon fiber layers. They evaluated also the damping properties of fiber-reinforced plates by using the finite element analysis [23]. For their studies, they used an iterative method to find the damping properties of the structure for some fixed orientation angle.

It was shown that the fiber orientation angle has a significant effect on the damping properties of the structure.

In this work, we developed first a finite element model using a zig-zag kinematic to analyze the damping properties of three layers (elastic orthotropic)/(viscoelastic orthotropic)/(elastic orthotropic) symmetric sandwich thin plates, as shown in Figure 1. Second, a numerical method is proposed to design viscoelastic composite structures with high damping. This method, based on asymptotic numerical method and automatic differentiation, permits to get damping properties as "analytical" function of the material fibers orientation. The variation of damping properties with face fibers orientation of some classical plate configurations will be presented and discussed.

2. A Model for Orthotropic Laminate Plate

Let us consider a three layer symmetric sandwich thin plate (elastic orthotropic)/(viscoelastic orthotropic)/(elastic orthotropic), as shown in Figure 1. The coordinate system (O, x, y, z) having the origin O at one corner is the global coordinates system. One denotes by z_i the ith middle plane coordinate with respect to $z = 0$. The external faces subscripted $i = 1, 3$ are elastic and orthotropic, while the middle layer subscripted $i = 2$ is viscoelastic and orthotropic. The thickness of the face layers is h_f and h_c for the core layer. The plate dimensions are L in the x-direction and l in the y-direction.

2.1. *Kinematics Model*

The damping of the structure is assumed to be induced thanks to large shear strain in the viscoelastic orthotropic layer as a direct consequence of the contrast between the elastic and viscoelastic layers. This large shear deformation must be modeled correctly in order to quantify accurately the increasing damping capacity of the sandwich plate. In this way, the kinematic analysis proposed here for the sandwich plate models the top and bottom faces using Kirchhoff–Love plate theory and the viscoelastic middle layer using Mindlin plate theory (see Figure 2). As is common to the authors [5, 8, 24, 25], the present analysis assumes the following:

- All points on a normal to the plate undergo the same transverse deflection.
- No slipping occurs at the interfaces between the three layers of the plate.
- All points on a normal to the undisturbed neutral plane of the top and bottom layers have the same rotation.
- The constitutive materials of the plate layers are homogeneous and isotropic. The Young/shear modulus of the viscoelastic core is complex frequency dependent, but the Poisson ratio is assumed to be constant.
- The top and bottom elastic layers have the same Young/shear modulus and the same mass density.

Based on these assumptions, the displacement field relationships associated to the classical Kirchhoff–Love plate theory are presented for the face layers:

$$\begin{cases} U_i(x, y, z, t) = u_i(x, y, t) - (z - z_i)w_{,x} \\ V_i(x, y, z, t) = v_i(x, y, t) - (z - z_i)w_{,y} \\ W_i(x, y, z, t) = w(x, y, t) \end{cases} \qquad i = 1, 3\ , \quad (1)$$

where u_i and v_i are in-plane displacements of the midplane of the ith layer and w is the common transverse displacement. The global reference $(O, \vec{X}, \vec{Y}, \vec{Z})$ coinciding with the midplane of the central layer leads to $z_2 = 0$ and $z_1 = -z_3 = (h_f + h_c)/2$.

And their deformation field is:

$$\{\xi_i\} = \{\Gamma_i\} + (z - z_i)\{\kappa\}, \quad (2)$$

where $\{\Gamma_i\}$ represents the linear strain tensor in membrane and $\{\kappa\}$ is the linear strain tensor in flexion.

The displacement field in the core layer, which is a viscoelastic layer, is written as: $i = 2$.

$$\begin{cases} U_2(x, y, z, t) = u(x, y, t) + z\,\beta_x(x, y, t) \\ V_2(x, y, z, t) = v(x, y, t) + z\,\beta_y(x, y, t) \\ W_2(x, y, z, t) = w(x, y, t) \end{cases}\ , \quad (3)$$

where u and v are the longitudinal displacement along the respective axes (Ox) and (Oy) of the mean plane of the core layer. β_x and β_y are the respective rotations about the axes (Oy) and (Ox) of the normal to the mean plane of the core layer.

Its deformation field is written as:

$$\{\xi_2\} = \{\Gamma_2\} + z\{\kappa_2\}. \tag{4}$$

The shear deformation field is written as:

$$\{\zeta_2\} = {}^t\{w_{,x} + \beta_x \quad w_{,y} + \beta_y\}. \tag{5}$$

2.2. *Generalized Forces*

Using the generalized Hooke's law, the normal forces N_i, the bending moments M_i, and the transverse shear forces Q_2 per unit length for each layer i are obtained:

$$\{N_i\} = {}^t\{N_{ixx} \quad N_{iyy} \quad N_{ixy}\} = [C_m]\{\Gamma_i\} \quad i = 1, 3, \tag{6}$$

$$\{M_i\} = {}^t\{M_{ixx} \quad M_{iyy} \quad M_{ixy}\} = [C_f]\{\kappa\} \quad i = 1, 3, \tag{7}$$

where $[C_m]$ and $[C_f]$ are, respectively, membrane and bending behavior matrices of orthotropic faces $i = 1,3$.

The viscoelastic behavior of the core is introduced using the classical convolution product [5], and the strain-stress of the plate leads to the following expressions of the normal N_2, transverse shear forces Q_2, and bending moment M_2 of the core layer $i = 2$:

$$\begin{cases} \{N_2\} = {}^t\{N_{2xx} \quad N_{2yy} \quad N_{2xy}\} = [C_{2m}]\{\Gamma_2\} \\ \{M_2\} = {}^t\{M_{2xx} \quad M_{2yy} \quad M_{2xy}\} = [C_{2f}]\{\kappa_2\} \\ \{Q_2\} = {}^t\{Q_{2xz} \quad Q_{2yz}\} = [C_{2s}]\{\zeta_2\} \end{cases}, \tag{8}$$

where $[C_{2m}]$, $[C_{2f}]$, and $[C_{2s}]$ are, respectively, membrane, bending, and transverse shear matrices of the core layer.

2.3. *Membrane, Bending, and Transverse Shear Expressions*

2.3.1. *For Elastic Faces*

The membrane matrix is decomposed into five elementary matrices simplifying the study of material orientation influence. To write those matrices, we define the following behavior constants:

$$c_{11} = \frac{h_f \times E_x}{1 - \nu_{xy}\nu_{yx}}, \; c_{22} = \frac{h_f \times E_y}{1 - \nu_{xy}\nu_{yx}}, \; c_{12} = \frac{h_f \times \nu_{yx} \times E_x}{1 - \nu_{xy}\nu_{yx}}$$
$$= \frac{h_f \times \nu_{xy} \times E_y}{1 - \nu_{xy}\nu_{yx}}, \; c_{66} = h_f \times G_{xy}. \tag{9}$$

The elementary matrices are now written with the behavior constants (9) as follows:

$$A_1 = \begin{bmatrix} c_{11} & c_{12} & 0 \\ c_{12} & c_{22} & 0 \\ 0 & 0 & c_{66} \end{bmatrix}, \tag{10a}$$

$$A_2 = \begin{bmatrix} c_{22} & c_{12} & 0 \\ c_{12} & c_{11} & 0 \\ 0 & 0 & c_{66} \end{bmatrix}, \tag{10b}$$

$$A_3 = \begin{bmatrix} 2(c_{12} + 2c_{66}) & c_{11} + c_{22} - 4c_{66} & 0 \\ c_{11} + c_{22} - 4c_{66} & 2(c_{12} + 2c_{66}) & 0 \\ 0 & 0 & c_{11} + c_{22} - 2(c_{12} + c_{66}) \end{bmatrix}, \tag{10c}$$

$$A_4 = \begin{bmatrix} 0 & 0 & c_{11} - c_{12} - 2c_{66} \\ 0 & 0 & c_{12} - c_{22} + 2c_{66} \\ c_{11} - c_{12} - 2c_{66} & c_{12} - c_{22} + 2c_{66} & 0 \end{bmatrix}, \tag{10d}$$

$$A_5 = \begin{bmatrix} 0 & 0 & c_{12} - c_{22} + 2c_{66} \\ 0 & 0 & c_{11} - c_{12} - 2c_{66} \\ c_{12} - c_{22} + 2c_{66} & c_{11} - c_{12} - 2c_{66} & 0 \end{bmatrix}. \tag{10e}$$

The fibers of the orthotropic material, which constitutes the face layers of the structure, are spotted in the global coordinate of the structure by the angle θ. This angle is defined as a plane rotation like $(\vec{X}, \vec{N_1}) = (\vec{Y}, \vec{N_2}) = \theta$, where the coordinate of the structure is $(O, \vec{X}, \vec{Y}, \vec{Z})$ and the local coordinate reference of the material is $(O, \vec{N_1}, \vec{N_2}, \vec{Z})$. The membrane matrix of the face layer is then determined as a function of the orientation angle θ.

$$C_m(\theta) = A_1 \cos^4(\theta) + A_2 \sin^4(\theta) + A_3 \sin^2(\theta)\cos^2(\theta) + A_4 \sin(\theta)\cos^3(\theta) + A_5 \sin^3(\theta)\cos(\theta). \tag{11}$$

The bending matrix of the face layers is linked to the membrane matrix by the formula:

$$C_f(\theta) = \frac{h_f^2}{12} C_m(\theta). \tag{12}$$

By setting the following constants:

$$B_i = \frac{h_f^2}{12} A_i, \quad i = 1, 2, 3, 4, 5. \tag{13}$$

The bending matrix Eq. (12) becomes:

$$C_f(\theta) = B_1 \cos^4(\theta) + B_2 \sin^4(\theta) + B_3 \sin^2(\theta)\cos^2(\theta) + B_4 \sin(\theta)\cos^3(\theta) + B_5 \sin^3(\theta)\cos(\theta). \tag{14}$$

2.3.2. *For Viscoelastic Core*

In a frequency domain, the complex and frequency dependent membrane and shear matrices of the viscoelastic core are, respectively, $\tilde{C}^*_{2m}$, $\tilde{C}^*_{2s}$ and are expressed as follows:

$$\tilde{C}^*_{2m} = \frac{h_c}{1-\nu_{xyc}\nu_{yxc}} \times \begin{bmatrix} E^*_{xc} & \nu_{yxc}\times E^*_{xc} & 0 \\ \nu_{yxc}\times E^*_{xc} & E^*_{yc} & 0 \\ 0 & 0 & (1-\nu_{xyc}\nu_{yxc})\times G^*_{xyc} \end{bmatrix}, \quad (15)$$

$$\tilde{C}^*_{2s} = h_c \begin{bmatrix} G^*_{xzc} & 0 \\ 0 & G^*_{yzc} \end{bmatrix}. \quad (16)$$

In the formulas (15) and (16), we impose the following assumptions: ν_{xyc}, ν_{yxc}, ν_{xzc}, ν_{yzc} are the real Poisson's ratio of the viscoelastic core.

The complex Young modulus E^*_{xc}, E^*_{yc} and the bulk modulus G^*_{xyc}, G^*_{xzc}, and G^*_{yzc} are decomposed into real and imaginary parts:

$$\begin{cases} E^*_{xc} = E_{0xc}(1+\mathrm{i}\eta_{xc}(\omega)) = E_{0xc} + E_{xc}(\omega) \\ E^*_{yc} = E_{0yc}(1+\mathrm{i}\eta_{yc}(\omega)) = E_{0yc} + E_{yc}(\omega) \\ G^*_{xyc} = G_{0xyc}(1+\mathrm{i}\eta_{xyc}(\omega)) = G_{0xyc} + G_{xyc}(\omega) \\ G^*_{xzc} = G_{0xzc}(1+\mathrm{i}\eta_{xzc}(\omega)) = G_{0xzc} + G_{xzc}(\omega) \\ G^*_{yzc} = G_{0yzc}(1+\mathrm{i}\eta_{yzc}(\omega)) = G_{0yzc} + G_{yzc}(\omega) \end{cases}. \quad (17)$$

This decomposition permits to write the membrane matrix $\tilde{C}^*_{2m}$ of the core as a sum of two parts: a constant and real part $\tilde{C}^0_{2m}$ and a complex frequency dependent part $\tilde{C}_{2m}(\omega)$ as follows:

$$\tilde{C}^*_{2m} = \frac{h_c}{1-\nu_{xyc}\nu_{yxc}} \begin{bmatrix} E_{0xc} & \nu_{yxc}\times E_{0xc} & 0 \\ \nu_{yxc}\times E_{0xc} & E_{0yc} & 0 \\ 0 & 0 & (1-\nu_{xyc}\nu_{yxc}) \times G_{0xyc} \end{bmatrix} + \frac{h_c}{1-\nu_{xyc}\nu_{yxc}} \begin{bmatrix} E_{xc}(\omega) & \nu_{yxc}\times E_{xc}(\omega) & 0 \\ \nu_{yxc}\times E_{xc}(\omega) & E_{yc}(\omega) & 0 \\ 0 & 0 & (1-\nu_{xyc}\nu_{yxc}) \times G_{0xyc}(\omega) \end{bmatrix}, \quad (18a)$$

$$\tilde{C}^*_{2m} = \tilde{C}^0_{2m} + \tilde{C}_{2m}(\omega), \quad (18b)$$

where the constant and real part is:

$$\tilde{C}^0_{2m} = \frac{h_c}{1-\nu_{xyc}\nu_{yxc}} \begin{bmatrix} E_{0xc} & \nu_{yxc}\times E_{0xc} & 0 \\ \nu_{yxc}\times E_{0xc} & E_{0yc} & 0 \\ 0 & 0 & (1-\nu_{xyc}\nu_{yxc}) \times G_{0xyc} \end{bmatrix}. \quad (18c)$$

And the complex and frequency dependent part is:

$$\tilde{C}_{2m}(\omega) = \frac{h_c}{1-\nu_{xyc}\nu_{yxc}} \times \begin{bmatrix} E_{xc}(\omega) & \nu_{yxc}\times E_{xc}(\omega) & 0 \\ \nu_{yxc}\times E_{xc}(\omega) & E_{yc}(\omega) & 0 \\ 0 & 0 & (1-\nu_{xyc}\nu_{yxc}) \times G_{xyc}(\omega) \end{bmatrix} \quad (18d)$$

Knowing that $\frac{E_{xc}}{\nu_{xyc}} = \frac{E_{yc}}{\nu_{yxc}}$, so $E_{yc} = \frac{\nu_{yxc}}{\nu_{xyc}} E_{xc}$.

The complex part of Eq. (18d) can be rewritten as follows:

$$\begin{cases} \tilde{C}_{2m}(\omega) = \dfrac{h_c}{1-\nu_{xyc}\nu_{yxc}} \begin{bmatrix} 1 & \nu_{yxc} & 0 \\ \nu_{yxc} & \nu_{yxc}/\nu_{xyc} & 0 \\ 0 & 0 & 0 \end{bmatrix} \\ \qquad E_{xc}(\omega) + \dfrac{h_c}{1-\nu_{xyc}\nu_{yxc}} \begin{bmatrix} 0 & 0 & 0 \\ 0 & 0 & 0 \\ 0 & 0 & (1-\nu_{xyc}\nu_{yxc}) \end{bmatrix} G_{xyc}(\omega). \\ \tilde{C}_{2m}(\omega) = \tilde{C}_{mE} E_{xc}(\omega) + \tilde{C}_{mG} G_{xyc}(\omega) \end{cases} \quad (18e)$$

The same decomposition is made for the shear matrix Eq. (16), which becomes:

$$\begin{cases} \tilde{C}^*_{2s} = h_c \begin{bmatrix} G_{0xzc} & 0 \\ 0 & G_{0yzc} \end{bmatrix} + h_c \begin{bmatrix} G_{xzc}(\omega) & 0 \\ 0 & G_{yzc}(\omega) \end{bmatrix}, \\ \tilde{C}^*_{2s} = \tilde{C}^0_{2s} + \tilde{C}_{2s}(\omega) \end{cases} \quad (19a)$$

where $\tilde{C}^0_{2s}$ and $\tilde{C}_{2s}(\omega)$ are, respectively, the real and complex part of $\tilde{C}^*_{2s}$:

$$\tilde{C}^0_{2s} = h_c \begin{bmatrix} G_{0xzc} & 0 \\ 0 & G_{0yzc} \end{bmatrix} \quad (19b)$$

and

$$\begin{cases} \tilde{C}_{2s}(\omega) = h_c \begin{bmatrix} G_{xzc}(\omega) & 0 \\ 0 & G_{yzc}(\omega) \end{bmatrix} = h_c \begin{bmatrix} 1 & 0 \\ 0 & 0 \end{bmatrix} G_{xzc}(\omega) \\ \qquad + h_c \begin{bmatrix} 0 & 0 \\ 0 & 1 \end{bmatrix} G_{yzc}(\omega). \\ \tilde{C}_{2s}(\omega) = \tilde{C}_{xG} G_{xzc}(\omega) + \tilde{C}_{yG} G_{yzc}(\omega) \end{cases} \quad (19c)$$

The material of the core being viscoelastic and orthotropic, its local coordinate reference is $(O, \overrightarrow{N^*_1}, \overrightarrow{N^*_2}, \overrightarrow{Z})$. The orientation of its fibers in the global coordinate reference is denoted α like: $(\overrightarrow{X}, \overrightarrow{N^*_1}) = (\overrightarrow{Y}, \overrightarrow{N^*_2}) = \alpha$.

When T_p and T_s denote the matrix of direction cosines of the coordinate transformation in plane and out of plane like:

$$\begin{cases} T_p = \begin{bmatrix} \cos^2(\alpha) & \sin^2(\alpha) & 2\sin(\alpha)\cos(\alpha) \\ \sin^2(\alpha) & \cos^2(\alpha) & -2\sin(\alpha)\cos(\alpha) \\ -\sin(\alpha)\cos(\alpha) & \sin(\alpha)\cos(\alpha) & \cos^2(\alpha)-\sin(\alpha) \end{bmatrix} \\ T_s = \begin{bmatrix} \cos(\alpha) & \sin(\alpha) \\ -\sin(\alpha) & \cos(\alpha) \end{bmatrix}. \end{cases} \quad (20)$$

We obtain for the core membrane and shear matrices the following expressions:

$$\begin{cases} C^0_{2m} = T_p \tilde{C}^0_{2m} T_p^{-1} \\ C_{2m}(\omega) = T_p \tilde{C}_{2m}(\omega) T_p^{-1} = T_p \tilde{C}_{mE} T_p^{-1} E_{xc}(\omega) \\ \qquad + T_p \tilde{C}_{mG} T_p^{-1} G_{xyc}(\omega) \\ C_{2m}(\omega) = C_{mE} E_{xc}(\omega) + C_{mG} G_{xyc}(\omega) \end{cases}, \tag{21}$$

$$\begin{cases} C^0_{2s} = T_s \tilde{C}^0_{2s} T_s^{-1} \\ C_{2s}(\omega) = T_s \tilde{C}_{2s} T_s^{-1} = T_s \tilde{C}_{xG} T_s^{-1} G_{xzc}(\omega) \\ \qquad + T_s \tilde{C}_{yG} T_s^{-1} G_{yzc}(\omega) \\ C_{2s}(\omega) = C_{xG} G_{xzc}(\omega) + C_{yG} G_{yzc}(\omega) \end{cases}. \tag{22}$$

3. Equation of Motion

The free vibration formulation of the plate is obtained by applying the Principle of Virtual Displacements (PVD). Assuming free vibration damping, we have:

$$\begin{cases} \delta P_{\text{int}} = -\iint_s \left(\sum_{i=1}^{3} {}^t\{N_i\}\{\delta\Gamma_i\} + \sum_{i=1,3} {}^t\{M_i\}\{\delta\kappa\} \right) ds \\ \qquad - \iint_s ({}^t\{M_2\}\{\delta_\kappa\} + {}^t\, Q_2 \delta\zeta_2) ds & (a) \\ \delta P_{ext} = 0 & (b) \\ \delta P_{acc} = \iint_s (2\rho_f h_f + \rho_c h_c) \dfrac{\partial}{\partial t} w \delta w ds & (c) \\ \delta P_{acc} = \delta P_{\text{int}} + \delta P_{ext} & (d) \end{cases}. \tag{23}$$

Note that in the present formulation, the in-plane and rotatory inertia effects are disregarded and only the transverse inertia effects are considered. Requiring the continuity of the displacement field at the interfaces between the three layers of the sandwich plate results in the following relationships:

$$\begin{cases} u_1 = u + \dfrac{h_c}{2}\beta_x - \dfrac{h_f}{2} w_{,x} \\ v_1 = v + \dfrac{h_c}{2}\beta_y - \dfrac{h_f}{2} w_{,y} \\ u_3 = u - \dfrac{h_c}{2}\beta_x + \dfrac{h_f}{2} w_{,x} \\ v_3 = v - \dfrac{h_c}{2}\beta_y + \dfrac{h_f}{2} w_{,y} \end{cases}. \tag{24}$$

This leads to reduce the components of the generalized displacement field vector to five independent functions $\{u, v, w, \beta_x, \beta_y\}$, which are related to the core. Thus, the membrane strain tensors are connected by the following relationships:

$$\begin{cases} \{\Gamma_1\} = \{\Gamma_2\} + \dfrac{h_c}{2}\{\kappa_2\} + \dfrac{h_f}{2}\{\kappa\} \\ \{\Gamma_3\} = \{\Gamma_2\} - \dfrac{h_c}{2}\{\kappa_2\} - \dfrac{h_f}{2}\{\kappa\} \end{cases}. \tag{25}$$

By introducing these interfaces conditions in Eq. (25), the variational formulation Eq. (23d) can be written with respect to the generalized displacements of the core:

$$\begin{aligned} \iint_s (2\rho_f h_f + \rho_c h_c) \frac{\partial^2}{\partial t^2} w \delta w ds &= -\iint_s ({}^t\{N\}\{\delta\Gamma_2\}) ds \\ &- \iint_s ({}^t\left\{M_2 + (N_1 - N_3) h_c/2\right\}\{\delta\kappa_2\}) ds \\ &- \iint_s ({}^t\left\{M_1 + M_3 + (N_1 - N_3) h_f/2\right\}\{\delta\kappa\} \\ &+ {}^t\{Q_2\}\{\delta\zeta_2\}) ds, \end{aligned} \tag{26}$$

where $\{N\} = \{N_1 + N_2 + N_3\}$ is the resultant of membrane forces of the three-layered plate. As the in-plane inertial terms and the axial forces are disregarded, the in-plane equilibrium equation is given by Daya et al. [25, 26]:

$$\iint_s {}^t\{N\}\{\delta\Gamma_2\} ds = 0, \tag{27}$$

where

$$\{N\} = 2[C_m]\{\Gamma_2\} + \left[C^*_{2m}\right]\{\Gamma_2\}, \tag{28}$$

and the flexural problem becomes:

$$\begin{aligned} &\iint_s (2\rho_f h_f + \rho_c h_c) \frac{\partial^2}{\partial t^2} w \delta w ds \\ &= -\iint_s ({}^t\left\{M_2 + (N_1 - N_3) h_c/2\right\}\{\delta\kappa_2\}) ds \\ &\quad - \iint_s ({}^t\left\{M_1 + M_3 + (N_1 - N_3) h_f/2\right\}\{\delta\kappa\} \\ &\quad + {}^t\left\{Q^*_{2s}\right\}\{\delta\zeta_2\}) ds, \end{aligned} \tag{29a}$$

$$\begin{aligned} &\iint_s (2\rho_f h_f + \rho_c h_c) \frac{\partial^2}{\partial t^2} w \delta w ds \\ &= -\iint_s ({}^t\left\{M^*_\beta\right\}\{\delta\kappa_2\} + {}^t\{M_w\}\{\delta\kappa\} + {}^t\left\{Q^*_{2s}\right\}\{\delta\zeta_2\}) ds. \end{aligned} \tag{29b}$$

By equaling Eq. (29a) to Eq. (29b), we deduce the expression:

$$\begin{aligned} \left\{M^*_\beta(\theta, \omega)\right\} &= \{M_2\} + \{N_1 - N_3\} h_c/2 \\ &= \left[C^*_{2f}(\omega)\right]\{\kappa_2\} + h_c[C_m(\theta)]\left(\tfrac{h_c}{2}\{\kappa_2\} + \tfrac{h_f}{2}\{\kappa\}\right), \end{aligned} \tag{30}$$

$$\{M_w(\theta)\} = \{M_1 + M_3\} + \{N_1 - N_3\} h_f/2 = 2\left[C_f(\theta)\right]\{\kappa\} + h_f\left[C_m(\theta)\right]\left(\frac{h_c}{2}\{\kappa_2\} + \frac{h_f}{2}\{\kappa\}\right), \tag{31}$$

and

$$\left\{Q^*_{2s}(\omega)\right\} = \left[C^*_{2s}(\omega)\right]\{\zeta_2\}. \tag{32}$$

Remembering that we have decomposed those matrices of the core into real and constant, and complex and frequency dependent, part above, we can also decompose $M^*_\beta(\theta, \omega)$ and $Q^*_{2s}(\omega)$ into the real and complex part. Thus,

$$\begin{cases} \left\{M^*_\beta(\theta,\omega)\right\} = \left\{M^0_\beta(\theta)\right\} + \left\{M_\beta(\omega)\right\} with & (a) \\ \left\{M^0_\beta(\theta)\right\} = \left[C^0_{2f}\right]\{\kappa_2\} + h_c\left[C_m(\theta)\right]\left(\frac{h_c}{2}\{\kappa_2\} + \frac{h_f}{2}\{\kappa\}\right) & (b) \\ \left\{M_\beta(\omega)\right\} = \left[C_{2f}(\omega)\right]\{\kappa_2\} & (c) \end{cases} \tag{33}$$

and

$$\begin{cases} \left\{Q_{2s}\right\} = \left\{Q^0_{2s} + Q_{2s}(\omega)\right\} \; with & (a) \\ \left\{Q^0_{2s}\right\} = \left[C^O_{2s}\right]\{\zeta_2\} & (b) \\ \left\{Q_{2s}(\omega)\right\} = \left[C_{2s}(\omega)\right]\{\zeta_2\} & (c) \end{cases}. \tag{34}$$

By introducing these decomposed matrices, Eqs. (31), (33a), and (34a) into the flexural problem Eq. (29b), we obtain:

$$\begin{aligned} &\iint_s (2\rho_f h_f + \rho_c h_c)\frac{\partial}{\partial t} w \delta w ds \\ &= -\iint_s \left({}^t\left\{M^0_\beta(\theta) + M_\beta(\omega)\right\}\{\delta\kappa_2\} + {}^t\{M_w(\theta)\}\{\delta\kappa\}\right) ds \\ &\quad - \iint_s \left({}^t\left\{Q^0_{2s} + Q_{2s}(\omega)\right\}\{\delta\zeta_2\}\right) ds. \end{aligned} \tag{35a}$$

By grouping the real part and the complex frequency dependent part Eq. (35a) becomes Eq. (35b) as below:

$$\begin{aligned} &\iint_s (2\rho_f h_f + \rho_c h_c)\frac{\partial}{\partial t} w \delta w ds \\ &= -\iint_s \left({}^t\left\{M^0_\beta(\theta)\right\}\{\delta\kappa_2\}\right) ds - \iint_s \left({}^t\{M_w(\theta)\}\{\delta\kappa\}\right) ds \\ &\quad - \iint_s \left({}^t\left\{Q^0_{2s}\right\}\{\delta\zeta_2\}\right) ds - \iint_s \left({}^t\left\{Q_{2s}(\omega)\right\}\{\delta\zeta_2\}\right) ds \\ &\quad - \iint_s \left({}^t\left\{M_\beta(\omega)\right\}\{\delta\kappa_2\}\right) ds. \end{aligned} \tag{35b}$$

4. Finite Element Discretization

To obtain the nonlinear complex eigenvalue problem given by the bending of the present model, finite element discretization is used. To do so, the two-dimensional four-node finite element is selected for the analysis. The transverse vibration study requires only five degrees of freedom per node: the transverse displacement (w), the slopes ($w_{,x}$, $w_{,y}$), and the rotations (B_x, B_y). Thus, for each element bounded by $k = 1, 2, 3, 4$, the element nodal displacement vector is:

$$\left\{U^e\right\} = {}^t\left\{w_k \; w_{,xk} \; w_{,yk} \; B_{xk} \; B_{yk}\right\}. \tag{36}$$

The element displacement vector is then written as follows:

$${}^t\left\{w \; B_x \; B_y\right\} = {}^t\left[N_w \; N_{\beta x} \; N_{\beta y}\right]\left\{U^e\right\}, \tag{37}$$

where $[N_w]$ is the matrix containing the classical cubic shape functions used for the interpolation of (w), while $[N_{\beta x}]$ and $[N_{\beta y}]$ are those containing the classical linear shape functions used for the interpolation of B_x and B_y, respectively [27].

Hence, these matrices are defined as:

$$\left[N_{wf}\right] = \begin{bmatrix} -N_{w,xx} \\ -N_{w,yy} \\ -2N_{w,xy} \end{bmatrix} \quad \left[N_{2f}\right] = \begin{bmatrix} N_{\beta x,x} \\ N_{\beta y,x} \\ N_{\beta x,y} + N_{\beta y,x} \end{bmatrix}$$
$$\left[N_{2s}\right] = \begin{bmatrix} N_{w,x} + N_{\beta x} \\ N_{w,y} + N_{\beta y} \end{bmatrix} \tag{38a}$$

and

$$\left[N_{wm}\right] = \frac{h}{2}\left[N_{2f}\right] + \frac{H}{2}\left[N_{wf}\right], \tag{38b}$$

which are 1×20 matrices of shape functions.

Therefore, those matrices in Eqs. (31), (33b), (33c), (34b), and (34c) are rewritten as follows:

$$\begin{cases} \left\{M^0_\beta(\theta)\right\} = \left[C^0_{2f}\right]\left[N_{2f}\right] + h\left[C_m(\theta)\right]\left[N_{wm}\right] & (a) \\ \{M_\beta(\omega)\} = \left[C_{2f}(\omega)\right]\left[N_{2f}\right] & (b) \\ \{M_w(\theta)\} = 2\left[C_f(\theta)\right]\left[N_{wf}\right] + H\left[C_m(\theta)\right]\left[N_{wm}\right] & (c) \\ \left\{Q^0_{2s}\right\} = \left[C^0_{2s}\right]\left[N_{2s}\right] & (d) \\ \left\{Q_{2s}(\omega)\right\} = \left[C_{2s}(\omega)\right]\left[N_{2s}\right] & (e) \end{cases}. \tag{39}$$

Doing so, the flexural problem Eq. (35b) becomes after finite element discretization and for one element:

$$\begin{aligned} -\omega \iint_{s_e} \left(\left(2\rho_f h_f + \rho h_c\right)^t\left[N_w\right]\left[N_w\right]\right) ds \\ = -\iint_{s_e} \left({}^t\left[N_{2f}\right]\left[C^0_{2f}\right]\left[N_{2f}\right]\right) ds \\ - \iint_{s_e} \left({}^t\left[N_{2s}\right]\left[C^0_{2s}\right]\left[N_{2s}\right]\right) ds \\ - \iint_{s_e} 2\left({}^t\left[N_{wf}\right]\left[C_f(\theta)\right]\left[N_{wf}\right]\right) ds \\ - \iint_{s_e} 2\left({}^t\left[N_{wm}\right]\left[C_m(\theta)\right]\left[N_{wm}\right]\right) ds \end{aligned}$$

$$-\iint_{s_e}\left({}^t\left[N_{2f}\right]\left[C_{2f}\left(\omega^2\right)\right]\left[N_{2f}\right]\right)ds$$
$$-\iint_{s_e}\left({}^t\left[N_{2s}\right]\left[C_{2s}\left(\omega^2\right)\right]\left[N_{2s}\right]\right)ds. \quad (40)$$

So, we have into the formula Eq. (40):
The elementary mass matrix:

$$\left[M^e\right]=\iint_{s_e}\left(\left(2\rho_f h_f+\rho h_c\right)^t\left[N_w\right]\left[N_w\right]\right)ds, \quad (41)$$

and elementary stiffness matrices:

$$\begin{cases}\left[K_2^e\right] &= \iint_{s_e}\left({}^t\left[N_{2f}\right]\left[C_{2f}^0\right]\left[N_{2f}\right]\right)ds \\ &\quad+\iint_{s_e}\left({}^t\left[N_{2s}\right]\left[C_{2s}^0\right]\left[N_{2s}\right]\right)ds \quad \text{(a)}\\ \left[K_1^e(\theta)\right] &= \iint_{s_e}2\left({}^t\left[N_{wf}\right]\left[C_f(\theta)\right]\left[N_{wf}\right]\right)ds \\ &\quad+\iint_{s_e}2\left({}^t\left[N_{wm}\right]\left[C_m(\theta)\right]\left[N_{wm}\right]\right)ds \quad \text{(b)}\\ \left[K^e(\omega)\right] &= \iint_{s_e}\left({}^t\left[N_{2f}\right]\left[C_{2f}(\omega)\right]\left[N_{2f}\right]\right)ds \\ &\quad+\iint_{s_e}\left({}^t\left[N_{2s}\right]\left[C_{2s}(\omega)\right]\left[N_{2s}\right]\right)ds \quad \text{(c)}\end{cases}. \quad (42)$$

Now we introduce the decomposed expression of behavior matrices Eq. (11) and Eq. (14) into Eq. (42b), so we have:

$$\begin{aligned}\left[K_1^e(\theta)\right]=&\left[\iint_{s_e}\left(2\left({}^t\left[N_{wf}\right]\left[B_1\right]\left[N_{wf}\right]\right)\right.\right.\\&\left.\left.+2\left({}^t\left[N_{wm}\right]\left[A_1\right]\left[N_{wm}\right]\right)\right)ds\right]\cos^4(\theta)\\&+\left[\iint_{s_e}\left(2\left({}^t\left[N_{wf}\right]\left[B_2\right]\left[N_{wf}\right]\right)\right.\right.\\&\left.\left.+2\left({}^t\left[N_{wm}\right]\left[A_2\right]\left[N_{wm}\right]\right)\right)ds\right]\sin^4(\theta)\\&+\left[\iint_{s_e}\left(2\left({}^t\left[N_{wf}\right]\left[B_3\right]\left[N_{wf}\right]\right)\right.\right.\\&\left.\left.+2\left({}^t\left[N_{wm}\right]\left[A_3\right]\left[N_{wm}\right]\right)\right)ds\right]\sin^2(\theta)\cos^2(\theta)\\&+\left[\iint_{s_e}\left(2\left({}^t\left[N_{wf}\right]\left[B_4\right]\left[N_{wf}\right]\right)\right.\right.\\&\left.\left.+2\left({}^t\left[N_{wm}\right]\left[A_4\right]\left[N_{wm}\right]\right)\right)ds\right]\sin(\theta)\cos^3(\theta)\\&+\left[\iint_{s_e}\left(2\left({}^t\left[N_{wf}\right]\left[B_5\right]\left[N_{wf}\right]\right)\right.\right.\\&\left.\left.+2\left({}^t\left[N_{wm}\right]\left[A_5\right]\left[N_{wm}\right]\right)\right)ds\right]\sin^3(\theta)\cos(\theta). \quad (43)\end{aligned}$$

In the formula (43) we set the constant stiffness as $\left[K_{1i}^e\right]\quad i=1,2,..,5$, so that we can write:

$$\begin{aligned}\left[K_1^e(\theta)\right]=&\left[K_{11}^e\right]\cos^4(\theta)+\left[K_{12}^e\right]\sin^4(\theta)\\&+\left[K_{13}^e\right]\sin^2(\theta)\cos^2(\theta)+\left[K_{14}^e\right]\sin(\theta)\cos^3(\theta)\\&+\left[K_{15}^e\right]\sin^3(\theta)\cos(\theta). \quad (44)\end{aligned}$$

In the same way, we introduce the decomposed expression of a core's matrices Eqs. (21) and (22) into Eq. (42c). We have, therefore,

$$\begin{aligned}\left[K^e(\omega)\right]=&\left[\iint_{s_e}\left({}^t\left[N_{2f}\right]\left[C_{mE}\right]\left[N_{2f}\right]\right)ds\right]E_{xc}(\omega)\\&+\left[\iint_{s_e}\left({}^t\left[N_{2f}\right]\left[C_{mG}\right]\left[N_{2f}\right]\right)ds\right]G_{xyc}(\omega)\\&+\left[\iint_{s_e}\left({}^t\left[N_{2s}\right]\left[C_{xG}\right]\left[N_{2s}\right]\right)ds\right]G_{xzc}(\omega)\\&+\left[\iint_{s_e}\left({}^t\left[N_{2s}\right]\left[C_{yG}\right]\left[N_{2s}\right]\right)ds\right]G_{yzc}(\omega). \quad (45)\end{aligned}$$

By setting the constant stiffness as $\left[K_i^e\right]\quad i=1,2,..,4$, the formula (45) becomes:

$$\begin{aligned}\left[K^e(\omega)\right]=&\left[K_1^e\right]E_{xc}(\omega)+\left[K_2^e\right]G_{xyc}(\omega)+\left[K_3^e\right]G_{xzc}(\omega)\\&+\left[K_4^e\right]G_{yzc}(\omega). \quad (46)\end{aligned}$$

The elementary nonlinear problem is now obtained as follows:

$$\left(\left[K_2^e\right]+\left[K_1^e(\theta)\right]+\left[K^e(\omega)\right]-\omega^2\left[M^e\right]\right)\left\{U^e\right\}=0. \quad (47)$$

Assembling these matrices yields the nonlinear complex eigenvalue problem, which is given as:

$$\left(\left[K_2\right]+\left[K_1(\theta)\right]+\left[K(\omega)\right]-\omega^2\left[M\right]\right)\left\{U\right\}=0. \quad (48)$$

In this nonlinear complex eigenvalue problem, we have:

$$\begin{aligned}\left[K_1(\theta)\right]=&\cos^4(\theta)\left[K_{r11}\right]+\sin^4(\theta)\left[K_{r12}\right]\\&+\sin^2(\theta)\cos^2(\theta)\left[K_{r13}\right]+\sin(\theta)\cos^3(\theta)\left[K_{r14}\right]\\&+\sin^3(\theta)\cos(\theta)\left[K_{r15}\right], \quad (49)\end{aligned}$$

$$\begin{aligned}\left[K(\omega)\right]=&\left[K_1\right]E_{xc}(\omega)+\left[K_2\right]G_{xyc}(\omega)+\left[K_3\right]G_{xzc}(\omega)\\&+\left[K_4\right]G_{yzc}(\omega). \quad (50)\end{aligned}$$

In formulas (49) and (50), matrices $\left[K_{1i}\right]\quad i=1,2,\ldots,5$ and $\left[K_i\right]\quad i=1,2,\ldots,4$ are, respectively, obtained by assembling the elementary ones $\left[K_{1i}^e\right]\quad i=1,2,..,5$ and $\left[K_i^e\right]\quad i=1,2,..,4$.

Table 1. Geometrical and mechanical characteristics of plates

Plates	Geometrical characteristics	Mechanical characteristics	
		Core layer	Faces layers
Rectangular plate with orthotropic faces and viscoelastic core (test 1)	$h_f = 0.406$ mm $h_c = 0.635$ mm $L = 1.829$ m $l = 1.219$ m	$E_1 = E_2 = 137\text{MP}a$ $G_{12} = 45.7\text{MP}a$ $G_{13} = 137\text{MP}a$ $G_{23} = 52.7\text{MP}a$ $\nu_{12} = 0.5$ $\rho = 124.1\text{Kg.m}^{-3}$	$E_f = 7.023 \times 10^{10}\text{P}a$ $\rho_f = 2820\ \text{Kg.m}^{-3}$ $\nu_f = 0.3$
Rectangular plate with orthotropic faces and viscoelastic core (test 2)	$h_f = 0.762$ mm $h_c = 0.254$ mm $L = 0.3$ m $l = 0.1$ m	$E_0 = 2670.08 \times 10^3\text{P}a$ $E = E_0(1 + 0.5i)$ $\rho_c = 999\text{Kg.m}^{-3}$ $\nu_c = 0.49$	$E_1 = 119\text{GP}a$ $E_2 = E_3 = 8.7\text{GP}a$ $G_{12} = G_{13} = 4\text{GP}a$ $G_{23} = 3\text{GP}a$ $\nu_{23} = 0.3$ $\nu_{12} = \nu_{13} = 0.32$ $\rho = 1560\ \text{Kg.m}^{-3}$
Square plate with orthotropic faces and viscoelastic core (test 3)	$h_f = 0.762$ mm $h_c = 0.254$ mm $L = l = 0.3$ m	$E_0 = 2670.08 \times 10^3\text{P}a$ $E = E_0(1 + 0.5i)$ $\rho_c = 999\text{Kg.m}^{-3}$ $\nu_c = 0.49$	$E_1 = 119\text{GP}a$ $E_2 = E_3 = 8.7\text{GP}a$ $G_{12} = G_{13} = 4\text{GP}a$ $G_{23} = 3\text{GP}a$ $\nu_{23} = 0.3$ $\nu_{12} = \nu_{13} = 0.32$ $\rho = 1560\ \text{Kg.m}^{-3}$

5. Complex Eigenvalue Problem and New Resolution Method

The general complex eigenvalue problem obtained by using the former developed method is used to study the variation of the damping properties of the structure according to the orientation angle θ of face layers. The purpose of this study is to find the good orientation of face layers, which can give the optimal damping properties of the structure. Here, we study only the case where the viscoelastic core has a constant complex modulus η. So, the general nonlinear eigenvalue problem to solve is simplified as given:

$$\left([K_2] + [K_1(\theta)] + [K(\eta)] - \omega^2 [M]\right)\{U\} = 0. \tag{51}$$

In this particular case we set for simplicity:

$$\begin{cases} [K_0] = [K_2] + [K(\eta)] \\ [K(\theta)] = [K_1(\theta)] \\ \omega^2 = \lambda \end{cases}. \tag{52}$$

This allows us to rewrite the general nonlinear eigenvalue problem at this form:

$$([K_0] + [K(\theta)] - \lambda [M])\{U\} = 0. \tag{53}$$

When θ is fixed, the complex eigenvalue problem is already studied by numerous authors [14, 15, 24]. In this article, we propose a new resolution procedure based on a path following

Table 2. Natural frequencies (Hz) for the undamped rectangular sandwich plate (ten first modes)

Modes	Present method	Alam et al. [29]	Araujo et al. [28]	Ferreira et al. (4×4Q9) [16]
1	22.90	23	23.5	23.28
2	43.64	44	44.8	44.91
3	70.67	69	71.7	70.93
4	77.97	78	79.5	83.04
5	90.36	90	92.5	91.72
6	123.20	123	126.5	128.90
7	124.85	126	126.8	139.28
8	149.36	143	150.7	151.62
9	168.00	162	170.7	171.56
10	168.48	172	173.0	181.46

Table 3. Frequencies and loss factors of simply supported rectangular plate ($\eta_e = 0.5$)

Angle θ		Mode 1		Mode 2		Mode 3	
		f_1	η_1	f_2	η_2	f_3	η_3
$\pi/2$	Present method	343.96	0.128	360.22	0.126	395.50	0.130
	Abaqus	339.24	0.150	358.27	0.130	396.03	0.122
$3\pi/8$	Present method	311.37	0.139	338.34	0.137	388.59	0.140
	Abaqus	306.34	0.158	336.47	0.141	389.31	0.133
$\pi/4$	Present method	243.76	0.164	302.21	0.155	389.30	0.149
	Abaqus	240.57	0.176	300.98	0.157	388.92	0.136
$\pi/8$	Present method	193.10	0.167	274.71	0.156	397.97	0.142
	Abaqus	191.50	0.175	273.66	0.158	396.77	0.134
0	Present method	172.56	0.168	249.38	0.171	396.54	0.132
	Abaqus	171.62	0.173	248.96	0.173	396.65	0.125

the method in which the face fiber orientation angle θ is the path parameter. The former well-posed path following the problem has to be solved by an appropriate method. We could use an incremental-iterative method like Newton–Raphson or the modified Newton method, but we preferred an asymptotic numerical method coupled with automatic differentiation that permits us to restrict the number of matrices to be inverted.

We set $\theta = \theta_j + \theta_r$, where θ_r is varying in the interval $[0, \theta_{r\,\max}]$ and θ_j is a starting point.

Then the unknowns, U and λ, are expanding as power series of θ_r:

$$\begin{cases} U(\theta) = U^j + \sum_{i=1}^{N} \theta_r^i U_i, & \left(U^j = U\left(\theta_j\right)\right) \\ \lambda(\theta) = \lambda^j + \sum_{i=1}^{N} \theta_r^i \lambda_i, & \left(\lambda^j = \lambda\left(\theta_j\right)\right) \end{cases}, \tag{54}$$

and the θ dependent stiffness $K(\theta)$ in Taylor series of θ_r:

$$\begin{aligned} K(\theta) &= \sum_{i=0}^{N} \frac{K^{(i)}(\theta_j)}{i!}\theta_r^i = K^j + \sum_{i=1}^{N} K_i \theta_r^i, \\ &\left(K^j = K\left(\theta_j\right), \quad K_i = \frac{K^{(i)}(\theta_j)}{i!} \quad i \geq 1\right), \\ K^j &= \cos^4(\theta_j)[K_{11}] + \sin^4(\theta_j)[K_{12}] + \sin^2(\theta_j)\cos^2(\theta_j)[K_{13}] \\ &\quad + \sin(\theta_j)\cos^3(\theta_j)[K_{14}] + \sin^3(\theta_j)\cos(\theta_j)[K_{15}], \end{aligned} \tag{55}$$

and

$$\begin{aligned} K_i = &\left(\frac{1}{i!}\left(2^{2i-3}\cos(4\theta_j + i\pi/2) + 2^{i-1}\cos(2\theta_j + i\pi/2)\right)\right)[K_{11}] \\ &+ \left(\frac{1}{i!}\left(2^{2i-3}\cos(4\theta_j + i\pi/2) - 2^{i-1}\cos(2\theta_j + i\pi/2)\right)\right)[K_{12}] \\ &+ \left(-\frac{2^{2i-3}}{i!}\cos(4\theta_j + i\pi/2)\right)[K_{13}] \qquad 1 \leq i \leq N \end{aligned}$$

Table 4. Frequencies and loss factors of clamped rectangular plate ($\eta_e = 0.5$)

Angle θ		Mode 1		Mode 2		Mode 3	
		f_1	η_1	f_2	η_2	f_3	η_3
$\pi/2$	Present method	690.88	0.0443	702.77	0.0474	726.40	0.0543
	Abaqus	683.36	0.0518	—	—	727.25	0.0581
$3\pi/8$	Present method	609.34	0.0536	627.84	0.0586	662.71	0.0677
	Abaqus	602.86	0.0594	623.74	0.0595	663.34	0.0662
$\pi/4$	Present method	430.79	0.0948	477.95	0.100	555.45	0.105
	Abaqus	427.84	0.1011	478.42	0.100	555.85	0.0954
$\pi/8$	Present method	306.59	0.164	389.39	0.141	519.78	0.120
	Abaqus	304.33	0.173	390.22	0.141	520.02	0.113
0	Present method	279.79	0.189	363.52	0.156	526.28	0.111
	Abaqus	278.07	0.198	363.64	0.156	527.48	0.106

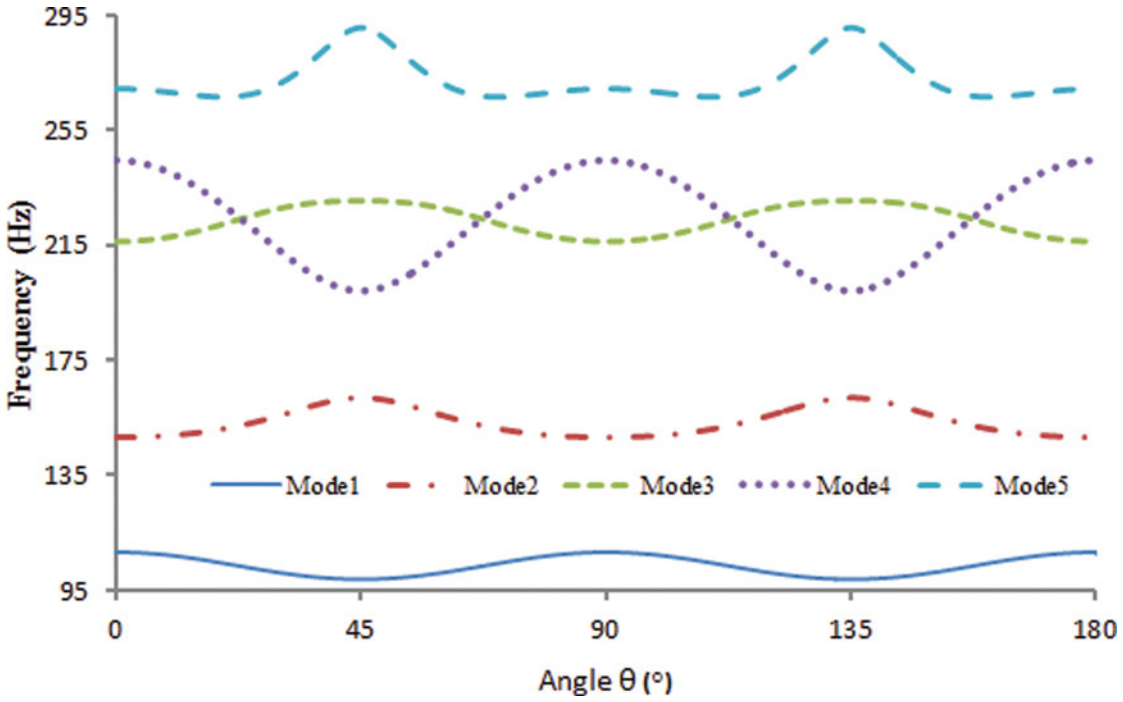

Fig. 3. Frequencies variation with θ for the first five modes of a CCCC square plate.

$$+\left(\frac{1}{i!}\left(2^{2i-3}\sin(4\theta_j+i\pi/2)+2^{i-2}\sin(2\theta_j+i\pi/2)\right)\right)[K_{14}]$$
$$+\left(\frac{1}{i!}\left(-2^{2i-3}\sin(4\theta_j+i\pi/2)+2^{i-2}\sin(2\theta_j+i\pi/2)\right)\right)[K_{15}], \quad (56)$$

where θ_j is the initial value of θ for each series.

Notice that j is an integer such that: $0 \le j \le j_{\max}$ and $\theta_{j=0} = 0, \theta_{j=j_{\max}} = \pi$. Inserting these series in the eigenproblem Eq. (53) we have:

$$\left[K_0 + K^j + \sum_{i=1}^{N}\theta_r^i K_i - \left(\lambda^j + \sum_{i=1}^{N}\theta_r^i\lambda_i\right)M\right] \times \left(U^j + \sum_{i=1}^{N}\theta_r^i U_i\right) = 0. \quad (57)$$

Developing and consolidating under the same exponent of θ_r, we obtain $(N+1)$ linear equations with $(2N)$ unknowns:

- In order 0:

$$\left(K_0 + K^j - \lambda^j M\right)U^j = 0. \quad (58a)$$

- In order 1:

$$\left(K_0 + K^j - \lambda^j M\right)U_1 = \lambda_1 MU^j - K_1 U^j. \quad (58b)$$

- In order $2 \le p \le N$:

$$\left(K_0 + K^j - \lambda^j M\right)U_p = \lambda_p MU^j - \sum_{i=1}^{p} K_i U_{p-i} + M\sum_{i=1}^{p-1}\lambda_i U_{p-i}. \quad (58b)$$

To these equations we add the eigenvectors (U_n) orthogonally condition ${}^tU^j \cdot U_n = 0$.

We obtain the generalized linear system in which unknowns are the pair (U_p, λ_p):

$$\begin{pmatrix} A & U^j \\ {}^tU^j & 0 \end{pmatrix}\begin{Bmatrix} U_p \\ \chi \end{Bmatrix} = \begin{Bmatrix} \lambda_p MU^j - \sum_{i=1}^{p} K_i U_{p-i} + M\sum_{i=1}^{p-1}\lambda_i U_{p-i} \\ 0 \end{Bmatrix}, \quad (3)$$

where χ denotes the Lagrange multiplier and the tangent matrix $[A] = (K_0 + K^j - \lambda^j M)$. The singularity of the tangent matrix $[A]$ entails that the system does not have a solution in the order p $(1 \le p \le N)$ without the solvency condition:

$${}^tU^j\left(\lambda_p MU^j - \sum_{i=1}^{p} K_i U_{p-i} + M\sum_{i=1}^{p-1}\lambda_i U_{p-i}\right) = 0. \quad (60a)$$

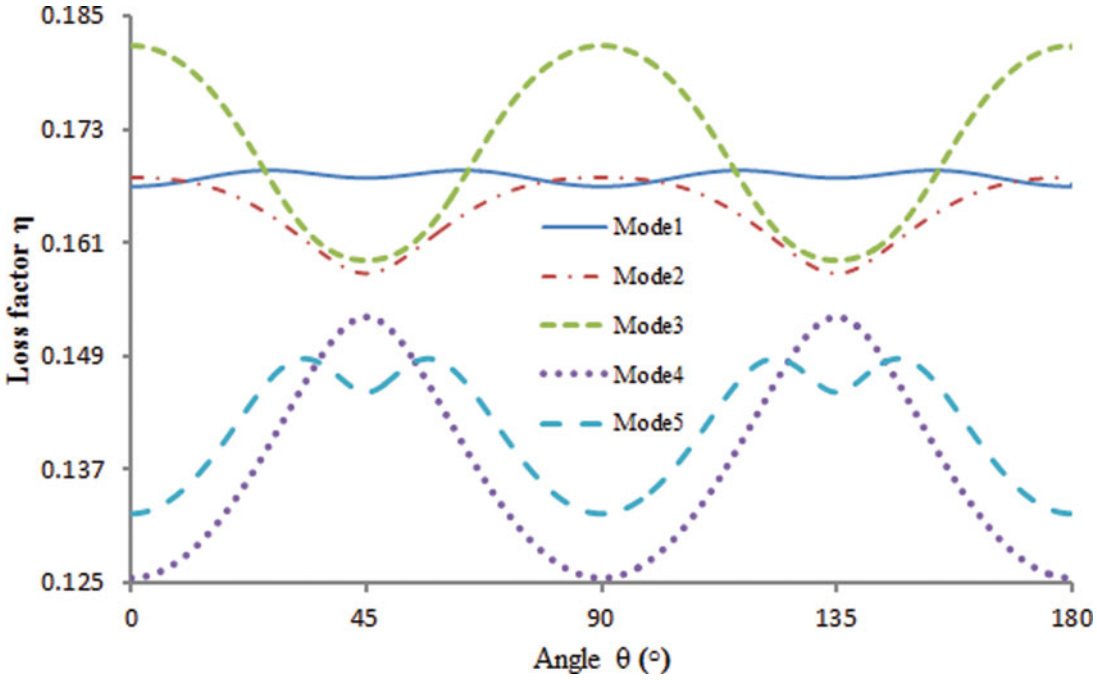

Fig. 4. Damping variation with θ for the first five modes of a CCCC square plate.

This solvency condition (60a) can be written accurately by a development:

$$\lambda_p^t U^j M U^j - {}^t U^j \sum_{i=1}^{p} K_i U_{p-i} + {}^t U^j M \sum_{i=1}^{p-1} \lambda_i U_{p-i} = 0. \tag{60b}$$

For each value of p terms of less than p index are known. From the solvency condition (60b), we obtain the value of λ_p as expressed:

$$\lambda_p = \frac{{}^t U^j \left(\sum_{i=1}^{p} K_i U_{p-i} - M \sum_{i=1}^{p-1} \lambda_i U_{p-i} \right)}{{}^t U^j M U^j} \qquad 1 \le p \le N. \tag{61}$$

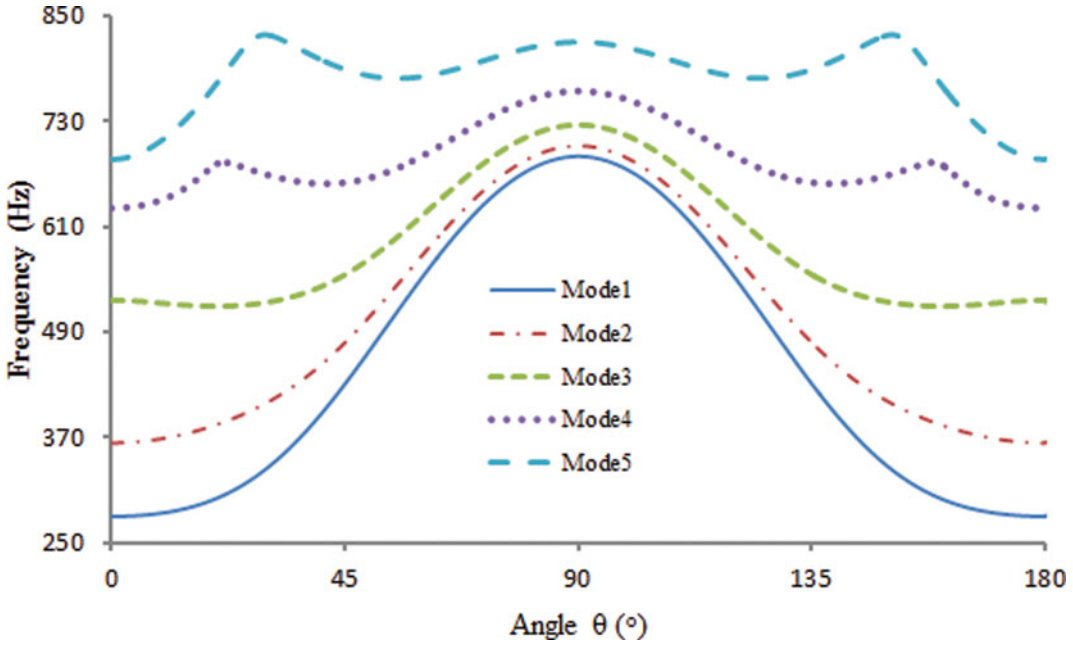

Fig. 5. Frequencies variation with θ for the first five modes of a CCCC rectangular plate.

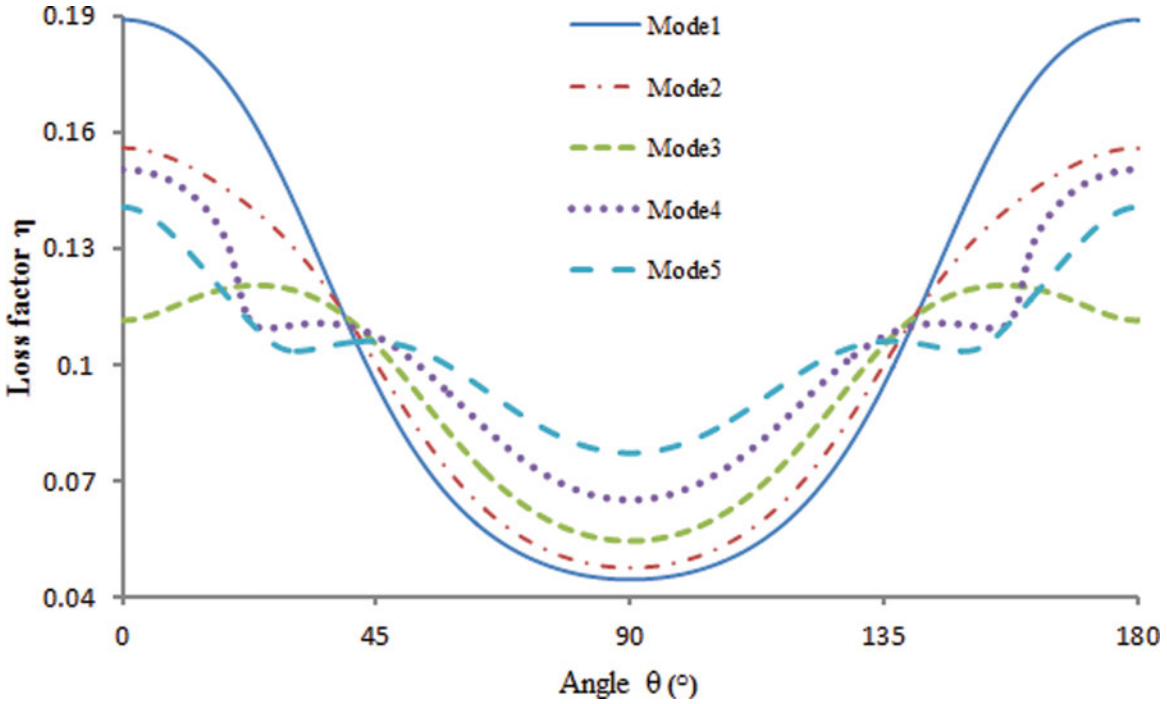

Fig. 6. Damping variation with θ for the first five modes of a CCCC rectangular plate.

Inserting the value of λ_p in the system Eq. (59), the second hand does not present any unknown; thus, by solving the system Eq. (59), we obtain the second unknown U_p.

In ANM, the last term U_N of the series is generally used to estimate the radius of convergence by requiring it to be very small compared to the first term U_1. So, the radius is:

$$\theta_{r\,\max} = \left(\varepsilon \frac{\| U_1 \|}{\| U_N \|}\right)^{\frac{1}{N-1}}, \tag{62}$$

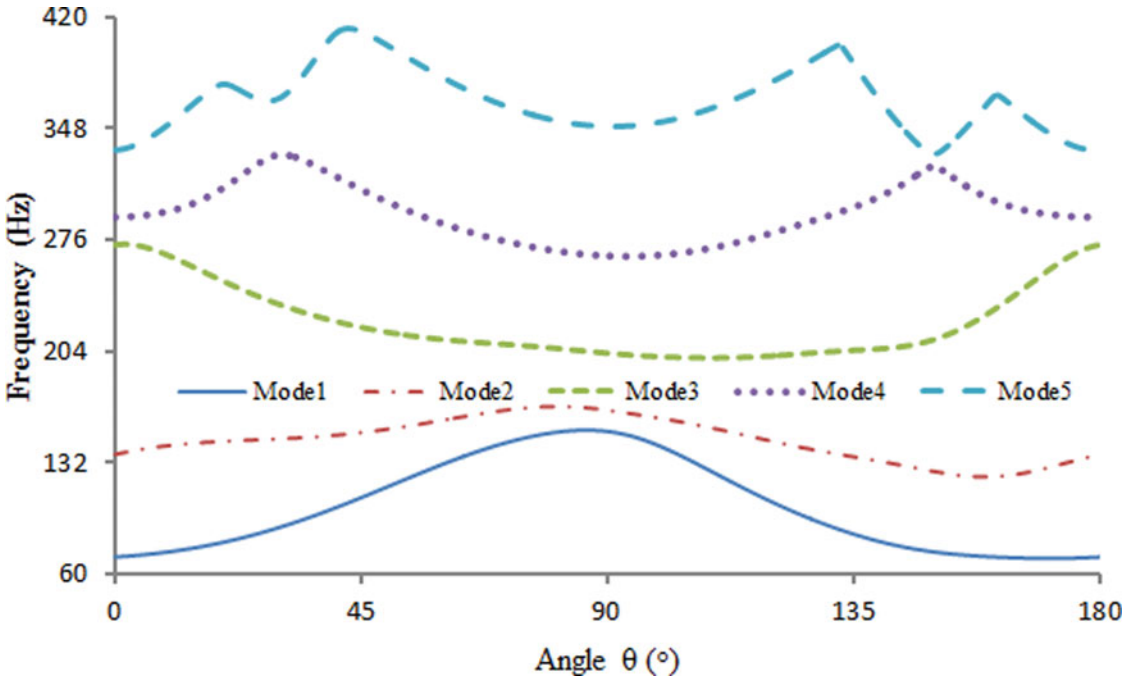

Fig. 7. Frequencies variation with θ for the first five modes of a CCFF rectangular plate.

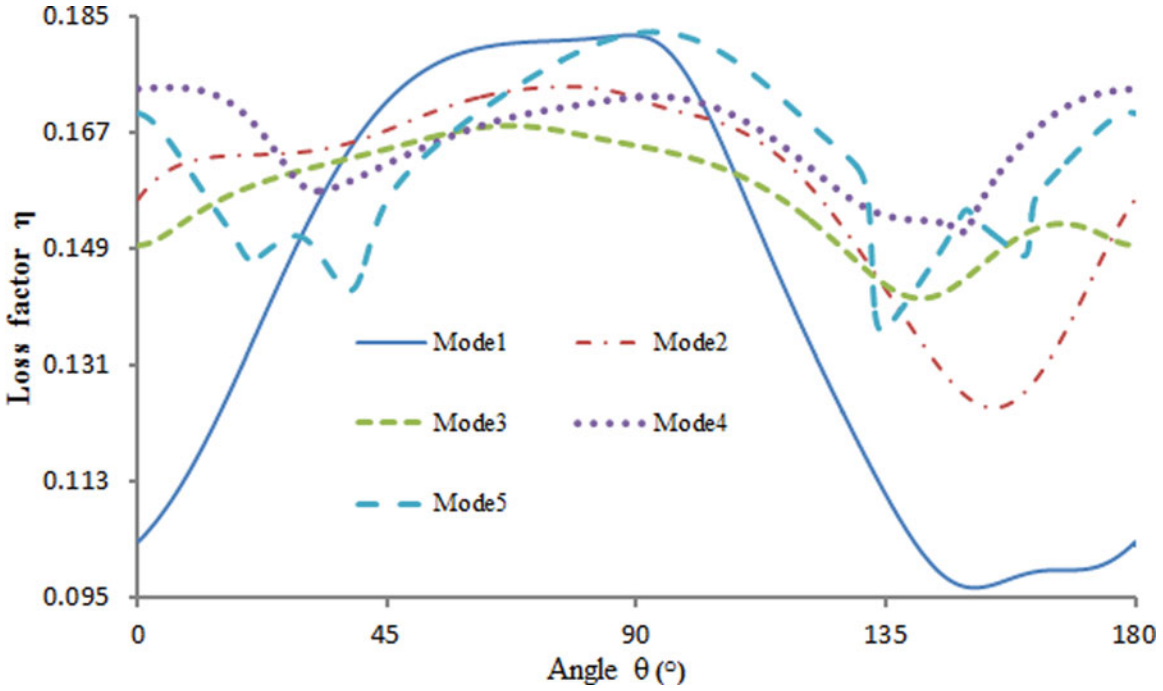

Fig. 8. Damping variation with θ for the first five modes of a CCFF rectangular plate.

where ε is a sufficiently small accuracy parameter (in practice, 10^{-4}s a good choice). Then we have to verify that $\theta_j \geq \pi$if this condition is not satisfied, then we set $\theta_j = \theta_j + \theta_{r\,\max}$ and restart the calculation from Eq. (59). More details about the continuation procedure can be found in [26].

6. Numerical Results

In this section, for the sake of validation and comparison, the developed model is first evaluated in two different cases, then we analyzed the variation of modal properties with the faces fiber orientation angle with two different plate configurations.

6.1. *Validation of the Proposed Finite Element Model*

The first test consists of a sandwich plate with isotropic faces and orthotropic core (Table 1), which is quite studied in the literature [16, 28, 29]. In Table 2, we can see that the results obtained with the proposed numerical finite element are in good agreement with the results in the literature [16, 28, 29].

In the second test, we considered an isotropic viscoelastic core with a constant complex modulus $E_c = E_0\,(1 + i\eta_c)$nd orthotropic faces with a varying θ fiber orientation angle (Table 1). Two boundary conditions have been considered for the rectangular plate: SSSS and CCCC. The results obtained with our sandwich plate finite element model (588 elements are used) are compared with a numerical model obtained on a commercial code Abaqus 6.7 (3600 elements C3D20R). A steady-state linear dynamic analysis is used on Abaqus 6.7 to monitor the linear response of the structure subjected to a continuous harmonic excitation. The damping is then obtained using the half-power bandwidth method. We observe in Tables 3 and 4 that the results obtained for the three first modes, with the developed model, are in good agreement with those obtained with the commercial code. One can, however, notice that some differences appear when the three first modes are relatively close (i.e., when $\theta = \pi/2$) but this is due to the limitation of the half-power bandwidth method.

6.2. *Study of the Damping Properties According to the Faces Fiber Orientation Angle*

In the first case, we show the continuous variation of the modal properties for a square plate (Table 1) according to the faces fiber orientation angle θ.

We can observe in Figures 3 and 4 that the orientation angle has few incidences on the modal properties when we consider CCCC boundary conditions for the plate. We can see here too that for each mode the maximum of damping will be obtained at different values of θ.

In the second case, we show the continuous variation of the modal properties for a rectangular plate (Table 1) according to the faces fiber orientation angle θ.

We can observe in Figures 5, 6, 7, and 8 that the orientation angle has a large incidence on the modal properties when we consider CCCC (Figures 5 and 6) or CCFF (Figures 7 and 8) boundary conditions. For each mode, the maximum of damping will be obtained in the same range of θ value.

7. Conclusion

In this work, a numerical method is developed to design orthotropic composite plates with a viscoelastic core. The finite element model is based on the first order zig-zag theory and

the numerical resolution of the free vibration problem is performed by the asymptotic numerical method and automatic differentiation technique. In this way, one obtains the damping properties (modal loss factors and natural frequencies) as "analytical" function of the material fibers orientation, which is useful to design composite structures with optimal damping.

References

[1] E.M. Kerwin, Damping of flexural waves by a constrained viscoelastic layer, J. Acous. Soc. Am., vol. 31, no. 7, pp. 952–962, 1959.

[2] R.A. DiTaranto and W. Blasingame, Composite damping of vibrating sandwich beams, J. Eng. Ind., vol. 89, no. B, pp. 633–638, 1967.

[3] B. Ma and J. He, A finite element analysis of viscoelastically damped sandwich plates, J. Sound Vib., vol. 152, no. 1, pp. 107–123, 1992.

[4] H. Boudaoud, E.M. Daya, S. Belouettar, L. Duigou, and M. Potier-Ferry, Damping analysis of beams submitted to passive and active control, Eng. Struct., vol. 31, no. 2, pp. 322–331, 2009.

[5] M. Bilasse, L. Azrar, and E.M. Daya, Complex modes based numerical analysis of viscoelastic sandwich plates vibrations, Comput. Struct., vol. 89, pp. 539–555, 2011.

[6] R. Rickards, A. Chate, and E. Barkanov, Finite element analysis fo damping the vibrations of laminated composites, Comput. Struct., vol. 47, pp. 1005–1015, 1993.

[7] K. Bathe and E.N. Dvorkin, On the automatic solution of nonlinear finite element equations, Comput. Struct., vol. 17, no. 5–6, pp. 871–879, 1983.

[8] X. Chen, H.L. Chen, and X.L. Hu, Damping prediction of sandwich structures by order-reduction-iteration approach, J. Sound Vib., vol. 222, no. 5, pp. 803–812, 1999.

[9] F. Abdoun, L. Azrar, E.M. Daya, and M. Potier-Ferry, Forced harmonic response of viscoelastic structures by an asymptotic numerical method, Comput. Struct., vol. 87, pp. 91–100, 2009.

[10] H. Boudaoud, S. Belouettar, E.M. Daya, and M. Potier-Ferry, A numerical method for nonlinear complex modes with application to active-passive damped sandwich structures, Eng. Struct., vol. 31, pp. 284–291, 2009.

[11] M. Bilasse, I. Charpentier, E.M. Daya, and Y. Koutsawa, A generic approach for the solution of nonlinear residual equations. Part II: Homotopy and complex nonlinear eigenvalue method, Comput. Meth. Appl. Mech. Eng., vol. 198, pp. 3999–4004, 2009.

[12] H. Hu, S. Belouettar, E.M. Daya, and M. Potier-Ferry, Evaluation of kinematic formulations for viscoelastically damped sandwich beam modeling, J. Sandwich Struct. Mater., vol. 8, pp. 477–495, 2006.

[13] E. Carrera, Historical review of zig-zag theories for multilayered plates and shells, Appl. Mech. Rev., vol. 56, no. 3, pp. 287–308, 2003.

[14] A.L. Araùjo, C.M. Mota Soares, C.A. Mota Soares, and J. Herskovits, Damping optimization of viscoelastic laminated sandwich composite structures, Struct. Multidiscip. Optim., vol. 39, pp. 569–579, 2009.

[15] A.L. Araùjo, C.M. Mota Soares, C.A. Mota Soares, and J. Herskovits, Optimal design and parameter estimation of frequency dependent viscoelastic laminated sandwich composite plates, Compos. Struct., vol. 92, pp. 2321–2327, 2010.

[16] A.J.M. Ferreira, A.L. Araùjo, A.M.A. Neves, J.D. Rodrigues, E. Carrera, and M. Cinefra, A finite element model using a unified formulation for analysis of viscoelastic sandwich laminates, Composites: Part B, vol. 45, pp. 1258–1264, 2013.

[17] E. Carrera, Developments, ideas, and evaluations based upon Reissner's mixed variational theorem in the modelling of multilayered plates and shells, Appl. Mech. Rev., vol. 54, pp. 301–309, 2001.

[18] E. Carrera, Evaluation of layer-wise mixed theories for laminated plate analysis, AIAA J., vol. 36, pp. 830–839, 1998.

[19] J.M. Berthelot and Y. Sefrani, Damping analysis of laminated beams and plates using the Ritz method, Compos. Struct., vol. 74, pp. 186–201, 2006.

[20] J.M. Berthelot and Y. Sefrani, Damping analysis of unidirectional glass and Kevlar fiber composites, Compos. Struct., vol. 64, pp. 27–51, 2004.

[21] J. Li and Y. Narita, Analysis and optimal design for the damping property of laminated viscoelastic plates under general edge conditions, Composites: Part B, vol. 45, pp. 972–980, 2013.

[22] R.D. Adams and M.R. Maheri, Dynamic flexural properties of anisotropic fibrous composite beams, Compos. Sci. Technol., vol. 50, pp. 497–514, 1994.

[23] M.R. Maheri and R.D. Adams, Finite element prediction of modal response of damped layered composite panels, Compos. Sci. Technol., vol. 55, pp. 13–23, 1995.

[24] M. Ganapathi, B.P. Patel, P. Boisse, and O. Polit, Flexural loss factors of sandwich and laminated composite beams using linear and nonlinear dynamic analysis, Composites: Part B, vol. 30, pp. 245–256, 1999.

[25] E.M. Daya, L. Azrar, and M. Potier-Ferry, An amplitude equation for the nonlinear vibration of viscoelastically damped sandwich beams, J. Sound Vib., vol. 271, no. 3–5, pp. 789–813, 2004.

[26] E.M. Daya and M. Potier-Ferry, A numerical method for nonlinear eigenvalue problems application to vibrations of viscoelastic structures, Comput. Struct., vol. 79, pp. 533–541, 2001.

[27] E.H. Boutyour, E.M. Daya, L. Azrar, and M. Potier-Ferry. An approximated harmonic balance method for nonlinear vibration of viscoelastic structures, J. Eng. Mater. Technol., vol. 128, no. 3, pp. 330–334, 2006.

[28] A.L. Araújo, C.M. Mota Soares, and C.A. Mota Soares, A viscoelastic sandwich finite element model for the analysis of passive, active and hybrid structures, Appl. Compos. Mater., vol. 17, pp. 529–42, 2010.

[29] N. Alam and N.T. Asnani, Vibration and damping analysis of multilayered rectangular plates with constrained viscoelastic layers, J. Sound Vib., vol. 97, pp. 597–614, 1984.